Atom Transfer Radical Polymerization in Miniemulsion: Partitioning Effects of Copper(I) and Copper(II) on Polymerization Rate, Livingness, and Molecular Weight Distribution†

Yasuyuki Kagawa,‡ Per B. Zetterlund,§ Hideto Minami,‡,§ and Masayoshi Okubo*,‡,§

Graduate School of Science and Technology, Kobe University, Kobe 657-8501, Japan, and Department of Chemical Science and Engineering, Faculty of Engineering, Kobe University, Kobe 657-8501, Japan

Received December 5, 2006; Revised Manuscript Received February 9, 2007

ABSTRACT: The effects of partitioning of Cu(I) and Cu(II) species to the aqueous medium on the polymerization rate (R_p), molecular weight and molecular weight distribution in the miniemulsion atom transfer radical polymerization system of styrene/CuBr/4,4′-dinonyl-2,2′-bipyridyl at 90 °C were investigated. According to both simulation (invoking the partitioning data for *n*-butyl methacrylate (*Macromolecules* **2000**, *33*, 7310−7320)) and experiment showed that the R_p and polydipersity (M_w/M_n) were higher in miniemulsion than in the corresponding solution polymerization as a result of a decrease in deactivator concentration (Cu(II) species) in the organic phase. Simulations indicated quantitatively that the increase in M_w/M_n was caused by (i) a decrease of activation−deactivation cycles and (ii) an increase of bimolecular termination.

Introduction

Controlled/living radical polymerization (CLRP) enables synthesis of polymers with predefined molecular weights (MW), narrow molecular weight distributions (MWD), and various complex architectures.[1,2] The most commonly employed CLRP techniques are nitroxide-mediated radical polymerization (NMP),[3] atom transfer radical polymerization (ATRP),[4,5] reversible addition−fragmentation chain transfer,[6] and recently also organotellurium-mediated radical polymerization.[7] In order for CLRP to realize its potential from an industrial perspective, it is essential that CLRP techniques compatible with polymerization in aqueous dispersed systems are developed, and recent years have seen significant progress in this area.[8−23] For example, we have recently reported the successful preparation of poly(isobutyl methacrylate)−polystyrene (P*i*BMA-*b*-PS) block copolymer particles in an aqueous medium by two-step ATRP.[8,9]

Heterogeneous radical polymerizations (emulsion, miniemulsion, microemulsion etc.) are considerably more complex than their homogeneous counterparts mainly due to partitioning of reactants (e.g., monomer, initiator) between the monomer and aqueous phases and compartmentalization.[24] In the case of CLRP, partitioning of deactivator to the aqueous medium is of particular concern.[21,25,26] This is exemplified in ATRP when the ligand is not sufficiently hydrophobic and/or the binding affinity toward the metal center is not strong enough, resulting in loss of control due to a significant fraction of the deactivator being located in the aqueous medium as opposed to the particles.[11,16,20] Hydrophobic ligands (e.g., 4,4′-dinonyl-2,2′-bipyridyl (dNbpy)) are therefore generally used to minimize exit of metal complexes to the aqueous phase, and under such conditions miniemulsion/emulsion ATRP proceeds satisfactorily.[8,9,11,16−21] However, even when hydrophobic ligands such as dNbpy are employed, significant partitioning of both Cu(I) and Cu(II) species may occur.[21] Qiu et al. measured the partitioning of Cu(I) and Cu(II) species (ligand: dNbpy) separately between *n*-butyl methacrylate (*n*BMA) and water using UV−vis spectroscopy,[21] revealing that as much as 20−30% of Cu(I) and 80−99% of Cu(II) species were located in the aqueous medium at 90 °C. However, in the reverse ATRP ab initio emulsion polymerization of *n*BMA, sufficient amounts of Cu(I) and Cu(II) species nonetheless remained in the monomer phase for the polymerization to proceed in a controlled/living manner.[21] Thus, it is apparent that partitioning of Cu(I) and Cu(II) species between the aqueous and organic phases is an important factor in ATRP in aqueous heterogeneous systems, but the effects of such partitioning on the kinetics have to date not been quantified.

Partitioning of nitroxide (deactivator) in aqueous heterogeneous NMP systems has also been reported.[27−29] Our previous theoretical investigations[26] have shown that nitroxide partitioning between the monomer and aqueous phases in miniemulsion NMP results in higher polymerization rate (R_p) and bimolecular termination rate in the pre-stationary state, but once the stationary state is reached, neither R_p nor the termination rate are affected by nitroxide partitioning. The time to reach the stationary state was very short in the case of S/2,2,6,6-tetramethylpiperidine-*N*-oxyl (TEMPO)/125 °C (<20 min, even using a relatively hydrophilic nitroxide like 4-hydroxy-2,2,6,6-tetramethylpiperidine-*N*-oxyl (OH-TEMPO)) compared to the time scale of the polymerization, and thus partitioning does not influence the polymerization kinetics except for in the very initial stage. It will be shown in the present paper that the same principles apply to ATRP in dispersed systems.

In the present paper, the effects of partitioning of Cu(I) and Cu(II) species between the organic and aqueous phases in the miniemulsion ATRP of styrene with CuBr/dNbpy at 90 °C have been investigated in detail. The corresponding solution polymerizations have been carried out in tandem with detailed kinetic modeling employing the software PREDICI[30] using experimentally obtained partitioning data,[21] thus enabling quantitative analysis of the effects of partitioning of Cu(I) and Cu(II) species.

† Part 288 of the series "Studies on Suspension and Emulsion".

* Corresponding author. Telephone/Fax: +81-78-803-6161. E-mail: okubo@kobe-u.ac.jp.

‡ Graduate School of Science and Technology, Kobe University.

§ Department of Chemical Science and Engineering, Faculty of Engineering, Kobe University.

10.1021/ma062786c CCC: $37.00
Published on Web 03/27/2007

Scheme 1

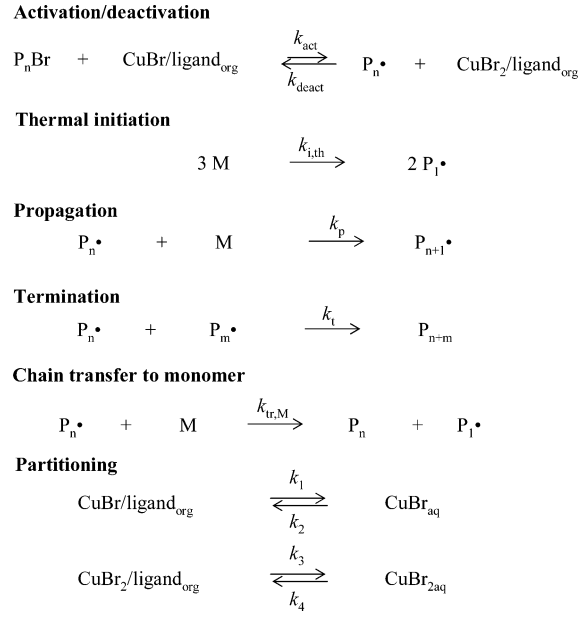

Partitioning of deactivator (Cu(II) species) to the aqueous phase results in higher R_p, but lower degree of control and livingness. Thus, it is important to quantitatively understand the effects of Cu(II) partitioning on the polymerization process in order to potentially develop systems where a suitable level of partitioning occurs, giving a higher R_p than in bulk/solution (a disadvantage of CLRP systems based on the persistent radical effect is the relatively low R_p), but still reasonable control and livingness.

Theory

Solution ATRP (Homogeneous System). ATRP in solution was modeled based on the generally accepted mechanism[2,5] (Scheme 1, without partitioning):

$$d[M]/dt = -k_p[P^\bullet][M] - k_{tr,M}[P^\bullet][M] - 3k_{i,th}[M]^3 \quad (1)$$

$$d[P^\bullet]/dt = k_{act}[PBr][CuBr] - k_{deact}[P^\bullet][CuBr_2] + k_{i,th}[M]^3 - 2k_t[P^\bullet]^2 \quad (2)$$

$$d[CuBr]/dt = -k_{act}[PBr][CuBr] + k_{deact}[P^\bullet][CuBr_2] \quad (3)$$

$$d[CuBr_2]/dt = k_{act}[PBr][CuBr] - k_{deact}[P^\bullet][CuBr_2] \quad (4)$$

$$d[PBr]/dt = -k_{act}[PBr][CuBr] + k_{deact}[P^\bullet][CuBr_2] \quad (5)$$

where PBr, P•, and M are alkyl halide, the propagating radical, and styrene monomer, respectively, and k_{act}, k_{deact}, $k_{i,th}$, k_t, k_p, and $k_{tr,M}$ are rate coefficients for activation, deactivation, thermal initiation, bimolecular termination, propagation, and chain transfer to monomer, respectively. The "2" in the mechanism for thermal initiation (Scheme 1) is included in $k_{i,th}$. The small radicals derived from chain transfer to monomer and thermal initiation as well as the ethyl 2-bromoisobutyrate (EB*i*B) radical were assumed to have equal reactivities, and were accounted for by the lumped parameter $P_1^\bullet$ (i.e., EB*i*B is represented by P_1Br in the model; see below for treatment of chain-length dependent propagation and termination). The above equations are simplifications of the actual equations that the software PREDICI[30] solves, which are based on each individual chain length (as apparent from eqs 6 − 8 below). All initial concentrations and rate coefficients are listed in Table 1.

Table 1. Input Parameters Used in Simulation for Atom Transfer Radical Polymerizations in Solution and Miniemulsion

input parameter	value	ref
temp (°C)	90	
$[styrene]_0$ (M)	4.36	
$[PBr]_0$ (M)	2.2×10^{-2}	
$[CuBr]_0$ (M)	4.4×10^{-2}	
k_{act} ($M^{-1}s^{-1}$)	0.19	41
k_{deact} ($M^{-1}s^{-1}$)	1.1×10^7	42
k_p ($M^{-1}s^{-1}$)	CLD[a]	31−35
k_t ($M^{-1}s^{-1}$)	CLD[a]	36−38
$k_{i,th}$ ($M^{-2}s^{-1}$)	5.79×10^{-12}	43
$k_{tr,M}$ ($M^{-1}s^{-1}$)	0.22	44
$\Gamma_{CuBr} = k_2/k_1$	3.2, ∞	21
$\Gamma_{CuBr_2} = k_4/k_3$	0.14, 1.0, ∞	21

[a] Chain-length dependent (see text for details)

Chain-length dependent propagation[31] was modeled according to the approach of Russell and Heuts:[32,33]

$$k_p^i = k_p^\infty\left[1 + C_1 \exp\left\{\frac{-\ln 2}{i_{1/2}}(i-1)\right\}\right]$$

$$C_1 = \frac{k_p^{\,1} - k_p^\infty}{k_p^\infty}; \quad i_{1/2} = \frac{k_p^i}{k_p^{i+1}} \quad (6)$$

where i denotes the degree of polymerization and k_p^∞ is the long-chain propagation rate coefficient. The parameter $i_{1/2}$ represents the increase in chain-length over which $k_p^i - k_p^\infty$ decreases by a factor of 2, and was taken to be the same as obtained experimentally for methyl methacrylate; $i_{1/2} = 1.12$.[32,34] On the basis of $k_p^1 = 8200\ M^{-1}\ s^{-1}$ at 75 °C and the activation energy of k_p^∞,[35] $k_p^1 = 1.32 \times 10^4\ M^{-1}\ s^{-1}$ and $k_p^\infty = 900\ M^{-1}\ s^{-1}$ at 90 °C.[35] The chain-length dependence of k_t was accounted for according to the composite model:[36,37]

$$k_t^{i,i} = \begin{cases} k_t^{1,1} \times i^{-0.5} & (i \le 100) \\ k_t^{1,1} \times 100^{-0.34} \times i^{-0.16} & (i > 100) \end{cases} \quad (7)$$

where $k_t^{i,i}$ is the termination rate coefficient between two propagating radicals of chain-length i, and $k_t^{1,1} = 1.3 \times 10^9\ M^{-1}\ s^{-1}$.[38] In the segmental diffusion region (i.e., "long chains"), the average experimental k_t ($\langle k_t \rangle$) for a mean chain length i is proportional to $i^{-0.16}$ for styrene.[37] For $i = 500$, eq 7 yields $k_t = 1 \times 10^8\ M^{-1}\ s^{-1}$, which is in good agreement with the experimentally (pulse laser polymerization) obtained $\langle k_t \rangle = 1.36 \times 10^8\ M^{-1}\ s^{-1}$ at 90 °C.[39] The cross-termination rate coefficients were obtained based on the geometric mean model:

$$k_t^{i,j} = (k_t^{i,i} k_t^{j,j})^{0.5} \quad (8)$$

Conversion dependences (i.e., dependence on the overall polymer weight fraction) of k_p and k_t (or any other rate coefficients in the model) were not included in the model. The weight fraction of polymer was kept below approximately 25% in all polymerizations (miniemulsion and solution) by the use of 50/50 styrene/toluene (organic phase) and conversions lower than 50%,[40] thereby rendering any such conversion effects negligible. The findings reported in the present paper are expected to apply also to the corresponding miniemulsion system in the absence of toluene at low conversion (i.e., for the same polymer weight fraction in the organic phase).

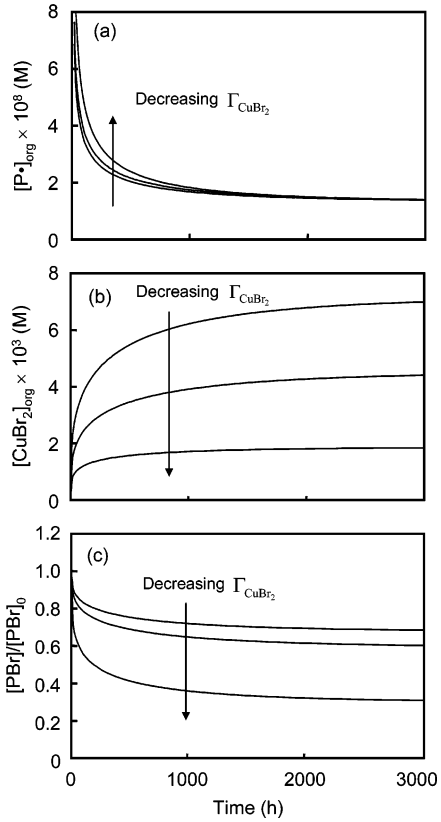

Figure 1. Simulated propagating radical concentration in organic phase ($[P^\bullet]_{org}$) (a), $[CuBr_2]_{org}$ (b), and fraction of "living" polymer ($[PBr]/[PBr]_0$) (c) as functions of polymerization time for atom transfer radical polymerization of styrene at 90 °C for 3000 h in miniemulsion ($[styrene]_0 = 4.36$ M, $[PBr]_0 = 0.022$ M, $[CuBr]_0 = 0.044$ M, [4,4′-dinonyl-2,2′-bipyridyl]$_0 = 0.088$ M) with thermal initiation based on constant [styrene] and rate of thermal initiation ($R_{i,th}$). Rate coefficients are listed in Table 1. Partitioning coefficients ($\Gamma_{CuBr} = [CuBr]_{org}/[CuBr]_{aq}$ and $\Gamma_{CuBr_2} = [CuBr_2]_{org}/[CuBr_2]_{aq}$): $\Gamma_{CuBr} = 3.2$ and $\Gamma_{CuBr_2} = 0.14$ or 1 (miniemulsion system), and $\Gamma_{CuBr} = \Gamma_{CuBr_2} = \infty$ (solution system).

Miniemulsion ATRP (Heterogeneous System). The miniemulsion system was modeled based on the following assumptions:

(i) The only phase transfer events are those involving Cu(I) and Cu(II) species.

Chain transfer to monomer followed by exit and reentry are significant kinetic events if the polymer particles are sufficiently small in conventional emulsion polymerization of styrene.[24] Considering the large particle diameters in this study ($d \approx 500$ nm), it was tentatively assumed that exit of radicals derived from chain transfer to monomer could be neglected.

(ii) The system is at phase equilibrium throughout the polymerization.

According to recent theoretical work,[45] phase equilibrium is reached very rapidly ($<10^{-4}$ s) under typical miniemulsion NMP conditions (referring to nitroxide partitioning). The partitioning data employed in the model were obtained in the absence of surfactant (see below);[21] it is possible that the surfactant influences both the partitioning and the rate at which phase transfer equilibrium is reached.

(iii) Compartmentalization effects are negligible.

It has been established that in order for compartmentalization effects to be significant in the case of styrene, a particle diameter of less than approximately 140 nm is required.[24,46] Considering that the particle diameter in the present study was approximately 500 nm, it is very unlikely that compartmentalization is exerting any significant influence on the kinetics.

Partitioning was modeled as depicted in Scheme 1, resulting in the following expressions for the partitioning coefficients (Γ):

$$\Gamma_{CuBr} = \frac{[CuBr]_{org}}{[CuBr]_{aq}} = \frac{k_2}{k_1} \quad (9)$$

$$\Gamma_{CuBr_2} = \frac{[CuBr_2]_{org}}{[CuBr_2]_{aq}} = \frac{k_4}{k_3} \quad (10)$$

where the subscripts "org" and "aq" denote organic and aqueous phases, respectively. The exit of Cu(I) to the aqueous phase results in an increase in the ratio of ligand/CuBr in the monomer droplets. However, it has been shown experimentally that increasing this ratio beyond 2 does not affect the rate of activation for the alkyl halide/CuBr/bipyridyl system (the initial ligand/CuBr ratio in the present system was 2).[47]

The partitioning ratios of Cu(I) and Cu(II) species between the organic and aqueous phases in the present system for *n*BMA at 90 °C were measured by Qiu et al. using UV−vis spectroscopy,[21] and these partitioning coefficients were used to model the present styrene system. As stated above, phase equilibrium at all times was assumed, and therefore the absolute values of k_1, k_2, k_3, and k_4 were selected arbitrarily such that Γ_{CuBr} and Γ_{CuBr_2} were in agreement with the experimental partitioning data by Qiu et al. (See Table 1.) The values employed were $k_1 = 2400$, $k_2 = 7600$, $k_3 = 8800$, and $k_4 = 1200$. The time to reach phase equilibrium is less than 2×10^{-3} s using these values.

Miniemulsion ATRP was thus modeled by the addition of new terms to eqs 3 and 4 to account for Cu(I) and Cu(II) partitioning:

$$d[P^\bullet]/dt = k_{act}[PBr][CuBr]_{org} - k_{deact}[P^\bullet][CuBr_2]_{org} + k_{i,th}[M]^3 - 2k_t[P^\bullet]^2 \quad (11)$$

$$d[CuBr]_{org}/dt = -k_{act}[PBr][CuBr]_{org} + k_{deact}[P^\bullet][CuBr_2]_{org} + k_2[CuBr]_{aq} - k_1[CuBr]_{org} \quad (12)$$

$$d[CuBr_2]_{org}/dt = k_{act}[PBr][CuBr]_{org} - k_{deact}[P^\bullet][CuBr_2]_{org} + k_4[CuBr_2]_{aq} - k_3[CuBr_2]_{org} \quad (13)$$

$$d[CuBr]_{aq}/dt = k_1[CuBr]_{org} - k_2[CuBr]_{aq} \quad (14)$$

$$d[CuBr_2]_{aq}/dt = k_3[CuBr_2]_{org} - k_4[CuBr_2]_{aq} \quad (15)$$

All modeling and simulations were implemented using the commercially available software package PREDICI (version 5.51, Computing in Technology GmbH, Germany).[30]

GPC traces suffer from band broadening ("axial dispersion"), i.e. the MWD derived from a GPC trace is somewhat broader than the "true" MWD of the polymer (even a perfectly monodisperse polymer would exhibit a distribution in the GPC MWD). This effect is particularly pronounced in the case of narrow MWDs. Before comparison of experimental and simulated MWDs, the simulated MWDs were therefore "corrected" for instrumental broadening[48−50] using the approach of Buback et al.[48] (eq 10 in ref 48, using $\sigma_v b = 0.1$)).

Experimental Section

Materials. Styrene was purified by distillation under reduced pressure in a nitrogen atmosphere. Deionized water with a specific resistance of 5×10^6 Ω·cm was distilled prior to use. EB*i*B (>98%, Tokyo Kasei Kogyo Co. Ltd., Tokyo, Japan), dNdpy (97%, Aldrich

Chem Co. Ltd.), CuBr (99%) and $CuBr_2$ (99%), toluene (99.5%), hexadecane (98%), and ascorbic acid (99.5%, Nacalai Tesque Inc., Kyoto, Japan) were used as received. Poly(vinyl alcohol) (PVA) was supplied by Nippon Synthetic Chemical Ind. Co. Ltd. (Gohsenol GH-17: degree of polymerization, 1700; degree of saponification, 88%).

Miniemulsion ATRP. Implementation of direct ATRP in miniemulsion is complicated by the fact that some extent of oxidation of CuBr during ultrasonication is inevitable. Comparison between miniemulsion and solution polymerizations is an integral part of the present work, and this would be rendered difficult by unknown levels of oxidation of CuBr in miniemulsion. Therefore, miniemulsion ATRP was carried out using activators generated by electron transfer[51,52] (AGET), during which copper species is initially present only in its higher oxidative state ($CuBr_2$). The typical procedure is as described below. EB*i*B (10 mg, 4.8×10^{-5} mol), $CuBr_2$ (21.4 mg, 9.6×10^{-5} mol), dNdpy (78.5 mg, 1.9×10^{-4} mol), toluene (1 g), and styrene (1 g, 9.6×10^{-3} mol) were mixed and heated in a sealed glass tube under nitrogen atmosphere at 70 °C until the mixture became homogeneous. This mixture was poured into a 1.25 wt % PVA aqueous solution (8 g), and subsequently ultrasonicated with a Ultrasonic Homogenizer (Nissei, US-600T) for 5 min in a ice−water bath. After ultrasonication, the miniemulsion was transferred to a glass ampule, degassed using several N_2/vacuum cycles, and subsequently an aqueous solution of ascorbic acid (ascorbic acid: 8.45 mg, 4.8×10^{-5} mol) was added under a N_2 atmosphere. The mixture was sealed off and shaken horizontally at a rate of 100 cycles/min at room temperature for 1 h to complete the reduction of $CuBr_2$ to CuBr. The ascorbic acid converts Cu(II) in the aqueous medium to Cu(I), which subsequently migrates into the organic phase in accordance with Γ_{CuBr}.[52] As Cu(II) in the aqueous medium disappears due to reaction with ascorbic acid, Cu(II) in the organic phase migrates to the aqueous medium to maintain phase equilibrium (Γ_{CuBr2}), ideally eventually resulting in complete depletion of Cu(II) species in both phases (during this process, the color of the emulsion changed from green (Cu(II)) to dark brown (Cu(I)). The glass ampules were subsequently immersed in a water bath at 90 °C (taken to be the start of the polymerizations, $t = 0$). Characterization (13.75 h miniemulsion polymerization): Conversion = 58%. Number-average molecular weight (M_n) = 30 240; Polydispersity (M_w/M_n) = 1.32

Solution ATRP. EB*i*B was added to a homogeneous solution of CuBr (13.7 mg, 9.6×10^{-5} mol), dNbpy, toluene, and styrene under nitrogen atmosphere, sealed off and immersed in a water bath at 90 °C (direct ATRP). Characterization (14.5 h solution polymerization): Conversion = 45%; M_n = 9470; M_w/M_n = 1.11.

Measurements. Conversions were measured by gas chromatography (GC-18A, Shimadzu Co., Kyoto, Japan) using injection and column temperatures of 220 and 120 °C, respectively (capillary column ULBON HR-20M, Shinwa Chem. Industries, Ltd.). Number-average particle diameters were obtained by dynamic light scattering (FPAR-1000RK, Otsuka Electronics Co. Ltd., Tokyo, Japan) using the Marquadt analysis routine. Molecular weights were measured by gel permeation chromatography (GPC) using two styrene/divinylbenzene gel columns (TOSOH Corporation, TSKgel GM-H_{HR}-H, 7.8 mm i.d × 30 cm, separation rate per column: approximately 50 to 4×10^8 g/mol (exclusion limit)) using tetrahydrofuran as eluent at 40 °C at a flow rate of 1.0 mL/min employing refractive index (TOSOH RI-8020/21). The columns were calibrated with six standard PS samples (1.05×10^3-5.48×10^6, M_w/M_n = 1.10−1.15). Theoretical molecular weights ($M_{n,th}$) were calculated according to $M_{n,th} = \alpha[M]_0 M_M/[I]_0$, where α is monomer conversion, $[M]_0$ and $[I]_0$ are the initial concentrations of monomer and initiator, respectively, and M_M is the molecular weight of monomer.

Results and Discussion

Simulations. In conventional radical polymerization, the stationary-state with respect to $[P\bullet]_{org}$ is normally reached within seconds. In CLRP, the time taken to reach the stationary state (t_{ss}) ranges between a few minutes and several hours, depending on the specific system.[2] The value of t_{ss} in the present direct ATRP system at 90 °C was estimated based on eq 16, which applies to the case of $[CuBr_2]_0 = 0$ with thermal initiation[2]

$$t_{ss} = \frac{(k_t K^2 I_0^2)^{1/2}}{3R_{i,th}^{3/2}} \tag{16}$$

where $K = k_{act}[CuBr]_0/k_{deact}$, I_0 is $[EBiB]_0$, and $R_{i,th}$ is the rate of thermal initiation. On the basis of the rate parameters in Table 1, one obtains t_{ss} = 1717 h. In other words, the polymerization proceeds exclusively in the pre-stationary state.

Simulations were initially carried out for a hypothetical scenario with constant [S] (= 4.36 M), $R_{i,th}$ (= 4.80×10^{-10} M s^{-1}), k_p (= 900 M^{-1} s^{-1}) and k_t (= 1.36×10^8 M^{-1} s^{-1}) based on eqs 9−15 to investigate the influence of partitioning on both the stationary and the pre-stationary state regimes. Simulations were carried out for $\Gamma_{CuBr} = 3.2$ and ∞ and $\Gamma_{CuBr_2} = 0.14$, 1, and ∞, where $\Gamma_{CuBr} = 3.2$ and $\Gamma_{CuBr_2} = 0.14$ correspond to the experimental partitioning data by Qiu et al.,[21] and $\Gamma_{CuBr_2} = 1$ and ∞ represent an intermediate value and solution conditions ($\Gamma_{CuBr} = \Gamma_{CuBr_2} = \infty$), respectively.

Parts a and b of Figure 1 show simulated $[P^\bullet]_{org}$ and $[CuBr_2]_{org}$ vs time for different values of Γ_{CuBr_2}. In the pre-stationary state, $[P^\bullet]_{org}$ increases with decreasing Γ_{CuBr_2}, whereas $[P^\bullet]_{org}$ is independent of Γ_{CuBr_2} in the stationary state. The values of $[CuBr_2]_{org}$ decrease with decreasing Γ_{CuBr_2} in both the stationary and the pre-stationary state. At phase equilibrium, the terms $k_2[CuBr]_{aq} - k_1[CuBr]_{org}$ and $k_4[CuBr_2]_{aq} - k_3[CuBr_2]_{org}$ are zero (eqs 12 and 13) and the system of differential equations reduces to that in solution, and consequently $[P^\bullet]_{org}$ is independent of the partitioning, consistent with our previous findings for the styrene/TEMPO (NMP) miniemulsion system at 125 °C.[26] In the pre-stationary state, some fraction of $CuBr_2$ escapes to the aqueous medium (i.e., there is net transfer of $CuBr_2$ to the aqueous phase before phase equilibrium has been reached), and the resulting reduction in $[CuBr_2]_{org}$ and accompanying reduction in deactivation rate leads to an increase in $[P^\bullet]_{org}$. The effect of CuBr partitioning is essentially the opposite of that of $CuBr_2$ partitioning, but due to the significantly higher water solubility of $CuBr_2$, the latter effect dominates. Simulations with $\Gamma_{CuBr} = 3.2$ and $\Gamma_{CuBr_2} = \infty$ revealed that the effect of CuBr partitioning on its own (resulting in 24% decrease in $[CuBr]_{org}$) is a reduction in $[P^\bullet]_{org}$ by less than 5% (data not shown).

Figure 1c shows the effect of Γ_{CuBr_2} on chain-end functionality, evaluated in terms of $[PBr]/[PBr]_0$, where [PBr] is monomeric and polymeric alkyl halide, and subscript 0 denotes the initial concentration. $[PBr]/[PBr]_0$ decreases with decreasing Γ_{CuBr_2} in the pre-stationary state because of increased termination rates caused by higher $[P^\bullet]_{org}$ (Figure 1a). However, $[P^\bullet]_{org}$ is independent of Γ_{CuBr_2} in the stationary state, and consequently the rate of loss of PBr is also unaffected by Γ_{CuBr_2}.

In the styrene/TEMPO miniemulsion system at 125 °C,[26] both $[P^\bullet]_{org}$ and $[TEMPO]_{org}$ are independent of Γ_{TEMPO} in the stationary state, whereas in the present ATRP miniemulsion system $[CuBr_2]_{org}$ deacreases with decreasing Γ_{CuBr_2} also in the stationary state. The reason for this difference is that in the styrene/TEMPO system at 125 °C, the alkoxyamine (dormant chains) concentration remains essentially constant over the simulation time, whereas in the present ATRP system, [PBr] decreases significantly with time and decreasing Γ_{CuBr_2} (Figure 1c). In the stationary state (both NMP and ATRP), $[P^\bullet]_{org}$ (and thus also R_p) is independent of the concentration of dormant

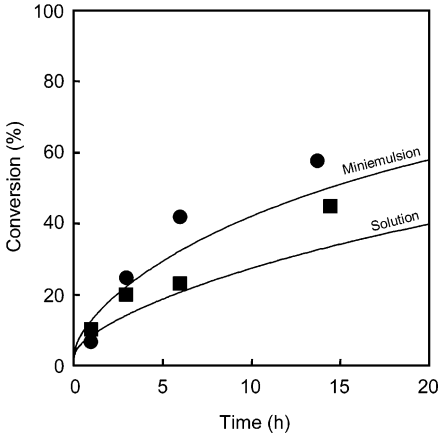

Figure 2. Simulated (solid lines) and experimental (■, ●) conversion vs time for atom transfer radical polymerization of styrene at 90 °C for 20 h in solution (■) and miniemulsion (●) ([styrene]$_0$ = 4.36 M, [PBr]$_0$ = 0.022 M, [CuBr]$_0$ = 0.044 M, [4,4′-dinonyl-2,2′-bipyridyl]$_0$ = 0.088 M). Rate coefficients for simulations are listed in Table 1. Partitioning coefficient (Γ_{CuBr} = [CuBr]$_{org}$/[CuBr]$_{aq}$ and Γ_{CuBr_2} = [CuBr$_2$]$_{org}$/[CuBr$_2$]$_{aq}$): Γ_{CuBr} = 3.2 and Γ_{CuBr_2} = 0.14 in miniemulsion.

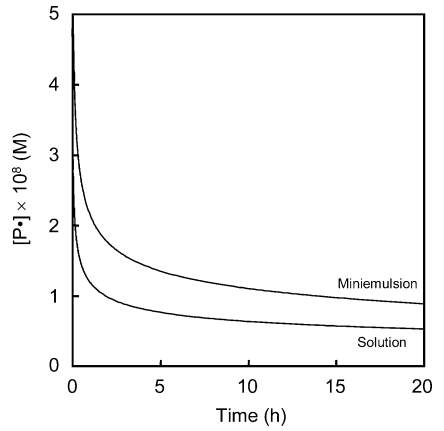

Figure 3. Simulated propagating radical concentrations in the organic phase ([P•]$_{org}$) as functions of polymerization time for atom transfer radical polymerization of styrene at 90 °C for 20 h in solution and miniemulsion ([styrene]$_0$ = 4.36 M, [PBr]$_0$ = 0.022 M, [CuBr]$_0$ = 0.044 M, [4,4′-dinonyl-2,2′-bipyridyl]$_0$ = 0.088 M). Rate coefficients are listed in Table 1. Partitioning coefficient (Γ_{CuBr} = [CuBr]$_{org}$/[CuBr]$_{aq}$ and Γ_{CuBr_2} = [CuBr$_2$]$_{org}$/[CuBr$_2$]$_{aq}$): Γ_{CuBr} = 3.2 and Γ_{CuBr_2} = 0.14 in miniemulsion.

chains ([P•]$_{org}$ = ($R_{i,th}$/2k_t)$^{1/2}$), whereas the deactivator concentration decreases with decreasing concentration of dormant chains.[2]

The present ATRP occurs exclusively in the pre-stationary state, and consequently, the experimentally obtained R_p would be significantly affected by Cu(I) and Cu(II) partitioning.

Comparison with Experiment. Figure 2 shows experimentally obtained conversion vs time data for the ATRP system styrene/CuBr/dNbpy at 90 °C in solution and miniemulsion, as well as the results of simulations of the same system based on eqs 1−15 using the Cu(I) and Cu(II) partitioning data of Qiu et al.[21] (Γ_{CuBr} = 3.2, Γ_{CuBr_2} = 0.14). The experimental data show that the miniemulsion polymerization was faster than the solution polymerization. Considering that the model employed in the simulations did not contain any adjustable parameters (all rate parameters were taken from the literature as listed in Table 1), the agreement between model and experiment in both solution and miniemulsion is indeed quite remarkable. The simulated [P•]$_{org}$ are shown in Figure 3, revealing how [P•]$_{org}$ is higher in miniemulsion than solution over the polymerization times investigated (by approximately a factor of 2), i.e., the polymerization proceeds in the pre-stationary state (see detailed explanation above). The simulated values of [P•]$_{org}$ in miniemulsion and solution at 20% conversion are 1.7 × 10^{-8} M and 7.4 × 10^{-9} M, respectively.

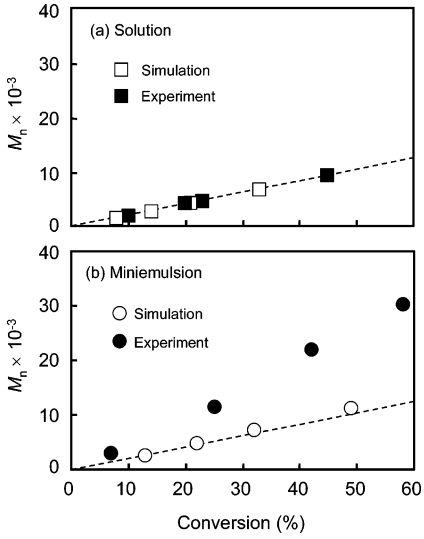

Figure 4. Simulated (□, ○) and experimental (■, ●) number-average molecular weight (M_n) for atom transfer radical polymerization of styrene at 90 °C in solution (a) (□, ■) and miniemulsion (b) (○, ●) ([styrene]$_0$ = 4.36 M, [PBr]$_0$ = 0.022 M, [CuBr]$_0$ = 0.044 M, [4,4′-dinonyl-2,2′-bipyridyl]$_0$ = 0.088 M). Broken lines are the theoretical molecular weight ($M_{n,th}$). Rate coefficients for simulations are listed in Table 1. Partitioning coefficient (Γ_{CuBr} = [CuBr]$_{org}$/[CuBr]$_{aq}$ and Γ_{CuBr_2} = [CuBr$_2$]$_{org}$/[CuBr$_2$]$_{aq}$): Γ_{CuBr} = 3.2 and Γ_{CuBr_2} = 0.14 in miniemulsion.

In the solution polymerization, both the simulated and the experimental M_n increased linearly with conversion (Figure 4a) in excellent agreement with the theoretical values ($M_{n,th}$). In miniemulsion (Figure 4b), the experimental M_n increased linearly with conversion, but the values were approximately twice as high as $M_{n,th}$. This suggests low initiation efficiency (= $M_{n,th}$/M_n), i.e., approximately half of the EB*i*B do not end up as polymer end groups but are lost in side reactions. There are previously reported cases of $M_n > M_{n,th}$ in direct ATRP (the situation is somewhat different in reverse ATRP) in miniemulsion/suspension.[16,25,53] This has been suggested to be caused by bimolecular termination between short radicals (also involving primary EB*i*B radicals) in the organic phase in the initial stage when [CuBr$_2$]$_{org}$ is low due to partitioning.[53,54] The simulated M_n were much lower than the experimental M_n, and only slightly higher than $M_{n,th}$. If bimolecular termination between short radicals were the only reason for the discrepancy between M_n and $M_{n,th}$, one would expect the simulations to also result in equally low initiation efficiency (because the mechanism responsible for low initiation efficiency is included in the model). The initiation efficiency ($M_{n,th}$/M_n) in the simulated miniemulsion polymerization was approximately 0.9, markedly higher than the experimental result ($M_{n,th}$/M_n = 0.4), throwing considerable doubt on this explanation. In other words, the miniemulsion simulations show that the initiation efficiency is reduced due to termination between short radicals; however, the effect is relatively small. The effect of partitioning of EB*i*B to the aqueous phase is expected to be negligible within this context. Thus, at present, a satisfactory explanation of the low initiation efficiency in miniemulsion remains elusive.

A reduction in initiation efficiency is equivalent to a reduction in [PBr], which in turn leads to lower R_p. Simulations under solution conditions with [EB*i*B]$_0$ reduced by a factor of 2 resulted in the conversion at 6 h decreasing from 20 to 17%, and R_p at 20% conversion decreasing by 18%. Thus, the R_p increases due to Cu(II) partitioning would in fact be counter-

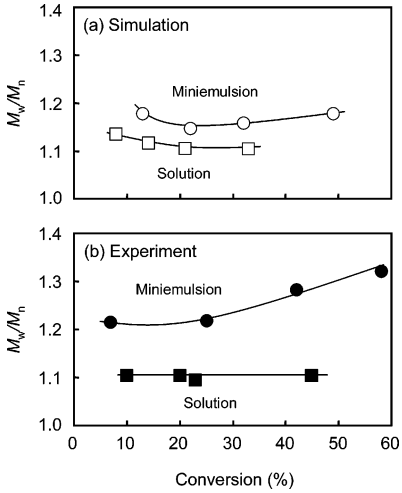

Figure 5. Simulated (○, □) (a) and experimental (●, ■) (b) polydispersity (M_w/M_n) for atom transfer radical polymerization of styrene at 90 °C in solution (□, ■) and miniemulsion (○, ●) ([styrene]$_0$ = 4.36 M, [PBr]$_0$ = 0.022 M, [CuBr]$_0$ = 0.044 M, [4,4′-dinonyl-2,2′-bipyridyl]$_0$ = 0.088 M). Rate coefficients for simulations are listed in Table 1. Partitioning coefficient ($\Gamma_{CuBr} = [CuBr]_{org}/[CuBr]_{aq}$ and $\Gamma_{CuBr_2} = [CuBr_2]_{org}/[CuBr_2]_{aq}$): $\Gamma_{CuBr} = 3.2$ and $\Gamma_{CuBr_2} = 0.14$ in miniemulsion. The lines are guides to the eye only.

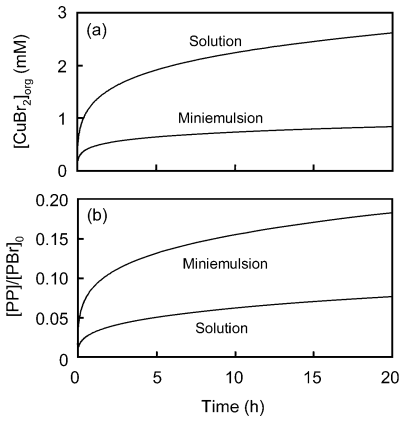

Figure 6. Simulated $[CuBr_2]_{org}$ (a) and fraction of dead polymer ($[PP]/[PBr]_0$) (b) for atom transfer radical polymerization of styrene at 90 °C in solution and miniemuslion ([styrene]$_0$ = 4.36 M, [PBr]$_0$ = 0.022 M, [CuBr]$_0$ = 0.044 M, [4,4′-dinonyl-2,2′-bipyridyl]$_0$ = 0.088 M). Rate coefficients are listed in Table 1. Partitioning coefficient ($\Gamma_{CuBr} = [CuBr]_{org}/[CuBr]_{aq}$ and $\Gamma_{CuBr_2} = [CuBr_2]_{org}/[CuBr_2]_{aq}$): $\Gamma_{CuBr} = 3.2$ and $\Gamma_{CuBr_2} = 0.14$ in miniemulsion.

acted to some extent by the effect of a lower [PBr] in miniemulsion.

Figure 5 shows the simulated and experimental M_w/M_n in solution and miniemulsion. According to both simulation and experiment, the M_w/M_n values were higher in miniemulsion than in solution. The higher M_w/M_n values in miniemulsion have two separate origins: (i) The number of activation−deactivation cycles (N_{cycles}) experienced by any given chain to reach a certain molecular weight is lower in miniemulsion than solution, due to lower $[CuBr]_{org}$ and $[CuBr_2]_{org}$ in miniemulsion. The polydispersity decreases with increasing N_{cycles} for a given molecular weight.[2] As shown in Figure 6a, $[CuBr_2]_{org}$ in miniemulsion is 2−3 times lower than in solution, and therefore a greater number of monomer units are incorporated into the chain per activation−deactivation cycle due to a reduction in the deactivation rate

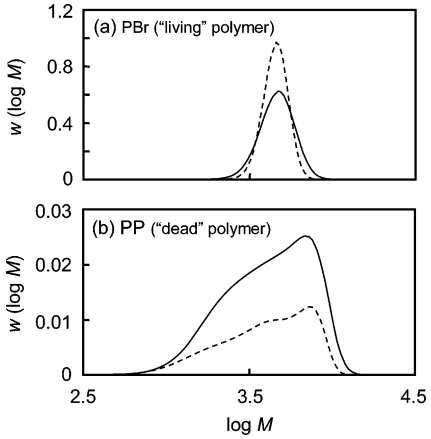

Figure 7. Simulated molecular weight distributions (MWDs) of "living" polymer (PBr) (a) and "dead" polymer (PP) (b) for atom transfer radical polymerization of styrene at 90 °C in solution (broken lines) and miniemulsion (solid lines) ([styrene]$_0$ = 4.36 M, [PBr]$_0$ = 0.022 M, [CuBr]$_0$ = 0.044 M, [4,4′-dinonyl-2,2′-bipyridyl]$_0$ = 0.088 M) at approximately 20% conversion. Rate coefficients are listed in Table 1. The MWDs (no broadening applied) correspond to properly normalized weight distributions; i.e., direct comparison of all four MWDs is possible.

(propagation competes with deactivation). The value of N_{cycles} is given by

$$N_{cycles} = \int_0^t k_{act}[CuBr]_{org}\,dt \qquad (17)$$

On the basis of the simulations for miniemulsion ($\Gamma_{CuBr} = 3.2$, $\Gamma_{CuBr_2} = 0.14$) and solution at $M_n \approx 4500$ (approximately 20% conversion), N_{cycles} = 48 in miniemulsion (t = 8200 s, 19% conversion, M_n = 4473) and 172 in solution (t = 21 600 s, 20% conversion, M_n = 4448). The considerably lower N_{cycles} in miniemulsion translates to an average number of styrene units added per activation−deactivation cycle of 0.9, to be compared with 0.25 in solution. (ii) $[P^\bullet]_{org}$ is higher in miniemulsion (Figures 2 and 3) due to $CuBr_2$ partitioning, which results in increased rates of termination and thus higher M_w/M_n. According to the simulations, the percentage of dead chains (by number) at 20 h is 18% in miniemulsion and 8% in solution (Figure 6b). Figure 7 shows separately the simulated MWDs of PBr ("living" polymer) and PP ("dead" polymer) in solution and miniemulsion at approximately 20% conversion. The corresponding weight distributions were normalized by adjusting the areas of the weight (=w(log M)/M) vs M plots to be proportional to the polymer mass in the respective system, prior to transformation to the displayed GPC (w(log M)) distributions.[55] The simulations reveal quantitatively that both points i and ii are responsible for the higher M_w/M_n in miniemulsion than in solution. The narrower MWD of PBr in solution (Figure 7a) is caused by N_{cycles} (solution) > N_{cycles} (miniemulsion), and the greater amount of the dead polymer by termination in miniemulsion is clearly visible in Figure 7b.

The significance of chain transfer to monomer in terms of the concentration of chains terminated by this mechanism ($[chain]_{tr,M}$) can be calculated according to eq 18[56]

$$[chain]_{tr,M} = \alpha[M]_0 C_{tr,M} \qquad (18)$$

where $C_{tr,M} = k_{tr,M}/k_p$, $[M]_0$ is the initial monomer concentration and α is the fractional conversion. At 60% conversion (close to the highest conversion in the present work), $k_{tr,M}$ = 0.22 M^{-1} s^{-1} gives (with k_p = 900 M^{-1} s^{-1})[35] $[chain]_{tr,M} = 6.4 \times 10^{-4}$ M. The total concentration of chains is approximately 0.043 M

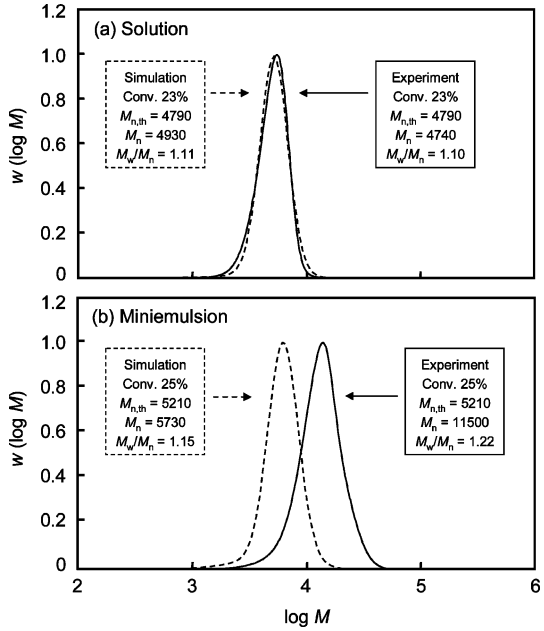

Figure 8. Simulated (broken lines, corrected for GPC broadening as detailed in text) and experimental (solid lines) molecular weight distributions (normalized to peak height) for atom transfer radical polymerization of styrene at 90 °C in solution (a) and miniemulsion (b) ($[\text{styrene}]_0 = 4.36$ M, $[\text{PBr}]_0 = 0.022$ M, $[\text{CuBr}]_0 = 0.044$ M, [4,4′-dinonyl-2,2′-bipyridyl]$_0 = 0.088$ M). Rate coefficients are listed in Table 1. Partitioning coefficient ($\Gamma_{\text{CuBr}} = [\text{CuBr}]_{\text{org}}/[\text{CuBr}]_{\text{aq}}$ and $\Gamma_{\text{CuBr}_2} = [\text{CuBr}_2]_{\text{org}}/[\text{CuBr}_2]_{\text{aq}}$): $\Gamma_{\text{CuBr}} = 3.2$ and $\Gamma_{\text{CuBr}_2} = 0.14$ in miniemulsion.

(based on the initial EB*i*B concentration), i.e. approximately 1.5% of chains have undergone chain transfer to monomer at 60% conversion. The contribution of chain transfer to monomer to loss of livingness is thus relatively insignificant in the present system.

Figure 8 shows the simulated and experimental MWDs (of total polymer, i.e., PBr + PP) in solution and miniemulsion. There is very good agreement between simulation and experiment in solution (Figure 8a). In miniemulsion (Figure 8b), the shapes of the simulated and experimental MWDs are similar (as expected based on the similar M_w/M_n values), but the experimental molecular weights are considerably higher than the simulated ones, consistent with $M_n > M_{n,th}$ in miniemulsion as discussed above.

Conclusions

The ATRP system styrene/CuBr/dNbpy in aqueous miniemulsion at 90 °C has been investigated with regards to the effects of partitioning of Cu(I) and Cu(II) species. Simulations based on the kinetic equations describing the system showed that R_p is independent of Cu(II) partitioning to the aqueous phase in the stationary state, but increases with increasing Cu(II) partitioning in the pre-stationary state. In the present system, the polymerization proceeds exclusively in the pre-stationary state, and there are thus significant partitioning effects.

The miniemulsion system yielded higher R_p and higher M_w/M_n than the corresponding solution polymerization. Simulations of both systems using PREDICI, based on experimentally obtained partitioning coefficients for Cu(I) and Cu(II) species and literature rate coefficients (no fitting parameters), revealed that the differences between the systems in terms of R_p and M_w/M_n can largely be explained as effects of partitioning. The particle size in the miniemulsion polymerizations was large enough (diameter ≈ 500 nm) for compartmentalization effects to be insignificant. Simulations also revealed that the higher M_w/M_n in miniemulsion than solution is a result of (i) a decrease in the number of activation−deactivation cycles experienced per chain during growth to a given chain length, and (ii) an increase of bimolecular termination. Both points i and ii are direct results of Cu(II) partitioning to the aqueous medium.

In the miniemulsion system, $M_n > M_{n,th}$ by close to a factor of 2 (initiation efficiency ≈ 0.4). This feature was present, but was much less pronounced (initiation efficiency ≈ 0.9), in the miniemulsion simulations. This casts some doubt on the previously proposed explanation[16,25,53] of excessive termination reactions at low conversion occurring due to lack of Cu(II) at the locus of polymerization (due to partitioning).

Acknowledgment. This work was partially supported by the Support Program for Start-ups from Universities (No. 1509) from the Japan Science and Technology Agency (JST), a Grant-in-Aid for Scientific Research (Grant 17750109) from the Japan Society for the Promotion of Science (JSPS), a Research Fellowship of the JSPS for Young Scientists (Y. K.), and a Kobe University Takuetsu-shita Research Project.

References and Notes

(1) Matyjaszewski, K. *Advances in Controlled/Living Radical Polymerization*; American Chemical Society: Washington, DC, 2003.
(2) Goto, A.; Fukuda, T. *Prog. Polym. Sci.* **2004**, *29*, 329−385.
(3) Hawker, C. J.; Bosman, A. W.; Harth, E. *Chem. Rev.* **2001**, *101*, 3661−3688.
(4) Kamigaito, M.; Ando, T.; Sawamoto, M. *Chem. Rev.* **2001**, *101*, 3689−3745.
(5) Matyjaszewski, K.; Xia, J. *Chem. Rev.* **2001**, *101*, 2921−2990.
(6) Moad, G.; Rizzardo, E.; Thang, S. H. *Aust. J. Chem.* **2005**, *58*, 379−410.
(7) Yamago, S. *J. Polym. Sci.; Part A: Polym. Chem.* **2006**, *44*, 1−12.
(8) Okubo, M.; Minami, H.; Zhou, J. *Colloid Polym. Sci.* **2004**, *282*, 747−752.
(9) Kagawa, Y.; Minami, H.; Okubo, M.; Zhou, J. *Polymer* **2005**, *46*, 1045−1049.
(10) Zetterlund, P. B.; Alam, M. N.; Minami, H.; Okubo, M. *Macromol. Rapid Commun.* **2005**, *26*, 955−960.
(11) Qiu, J.; Charleux, B.; Matyjaszewski, K. *Prog. Polym. Sci.* **2001**, *26*, 2083−2134.
(12) Cunningham, M. F. *Prog. Polym. Sci.* **2002**, *27*, 1039−1067.
(13) Nishikawa, T.; Kamigaito, M.; Sawamoto, M. *Macromolecules* **1999**, *32*, 2204−2209.
(14) Nicolas, J.; Charleux, B.; Guerret, O.; Magnet, S. P. *Angew. Chem., Int. Ed.* **2004**, *43*, 6186−6189.
(15) Ferguson, C. J.; Hughes, R. J.; Nguyen, D.; Pham, B. T. T.; Gilbert, R. G.; Serelis, A. K.; Such, C. H.; Hawkett, B. S. *Macromolecules* **2005**, *38*, 2191−2204.
(16) Matyjaszewski, K.; Qiu, J.; Shipp, D. A.; Gaynor, S. G. *Macromol. Symp.* **2000**, *155*, 15−29.
(17) Eslami, H.; Zhu, S. *Polymer* **2005**, *46*, 5484−5493.
(18) Simms, R. Y.; Cunningham, M. F. *J. Polym. Sci., Part A: Polym. Chem.* **2006**, *44*, 1628−1634.
(19) Li, M.; Matyjaszewski, K. *J. Polym. Sci., Part A: Polym. Chem* **2003**, *41*, 3606−3614.
(20) Li, M.; Min, K.; Matyjaszewski, K. *Macromolecules* **2004**, *37*, 2106−2112.
(21) Qiu, J.; Pintauer, T.; Gaynor, S. G.; Matyjaszewski, K.; Charleux, B.; Vairon, J.-P. *Macromolecules* **2000**, *33*, 7310−7320.
(22) Save, M.; Guillaneuf, Y.; Gilbert, R. G. *Aust. J. Chem.* **2006**, *59*, 693−711.
(23) Delaittre, G.; Nicolas, J.; Lefay, C.; Save, M.; Charleux, B. *Chem. Commun.* **2005**, *5*, 614.
(24) Gilbert, R. G. *Emulsion Polymerization: A Mechanistic Approach*; Academic Press: London, 1995.
(25) Matyjaszewski, K.; Qui, J.; Tsarevsky, N. V.; Charleux, B. *J. Polym. Sci., Part A: Polym. Chem.* **2000**, *38*, 4724−4734.
(26) Zetterlund, P. B.; Okubo, M. *Macromol. Theory Simul.* **2005**, *14*, 415−420.
(27) Tortosa, K.; Smith, J. A.; Cunningham, M. F. *Macromol. Rapid Commun.* **2001**, *22*, 957−961.
(28) Ma, J. W.; Smith, J. A.; McAuley, K. B.; Cunningham, M. F.; Keoshkerian, B.; Georges, M. K. *Chem. Eng. Sci.* **2003**, *58*, 1163−1176.

(29) Farcet, C.; Nicolas, J.; Charleux, B. *J. Polym. Sci., Part A: Polym. Chem.* **2002**, *40*, 4410−4420.
(30) Wulkow, M. *Macromol. Theory Simul.* **1996**, *5*, 393−416.
(31) Zetterlund, P. B.; Busfield, W. K.; Jenkins, I. D. *Macromolecules* **2002**, *35*, 7232−7237.
(32) Smith, G. B.; Russell, G. T.; Yin, M.; Heuts, J. P. A. *Eur. Polym. J.* **2005**, *41*, 225−230.
(33) Heuts, J. P. A.; Russell, G. T. *Eur. Polym. J.* **2006**, *42*, 3−20.
(34) Willemse, R. X. E.; Staal, B. B.; van-Herk, A. M.; Pierik, S. C. J.; Klumperman, B. *Macromolecules* **2003**, *36*, 9797−9803.
(35) Buback, M.; Gilbert, R. G.; Hutchinson, R. A.; Klumperman, B.; Kuchta, F. D.; Manders, B. G.; O'Driscoll, K. F.; Russell, G. T.; Schweer, J. *Macromol. Chem. Phys.* **1995**, *196*, 3267−3280.
(36) Smith, G. B.; Russell, G. T.; Heuts, J. P. A. *Macromol. Theory Simul.* **2003**, *12*, 299−314.
(37) Olaj, O. F.; Vana, P. *Macromol. Rapid Commun.* **1998**, *19*, 433−439.
(38) Russell, G. T. *Aust. J. Chem.* **2002**, *55*, 399−414.
(39) Beuermann, S.; Buback, M. *Prog. Polym. Sci.* **2002**, *27*, 191−254.
(40) Zetterlund, P. B.; Yamauchi, S.; Yamada, B. *Macromol. Chem. Phys.* **2004**, *205*, 778−785.
(41) Goto, A.; Fukuda, T. *Macromol. Rapid Commun.* **1999**, *20*, 633−636.
(42) Ohno, K.; Goto, A.; Fukuda, T.; Xia, J.; Matyjaszewski, K. *Macromolecules* **1998**, *31*, 2699−2701.
(43) Hui, A. W.; Hamielec, A. E. *J. Appl. Polym. Sci.* **1972**, *16*, 749−769.
(44) Shipp, D. A.; Matyjaszewski, K. *Macromolecules* **1999**, *32*, 2948−2955.
(45) Ma, J. W.; Cunningham, M. F.; McAuley, K. B.; Keoshkerian, B.; Georges, M. K. *Macromol. Theory Simul.* **2002**, *11*, 953−960.
(46) Casey, B. S.; Morrison, B. R.; Maxwell, I. A.; Gilbert, R. G.; Napper, D. H. *J. Polym. Sci., Part A: Polym. Chem.* **1994**, *32*, 605−630.
(47) Nanda, A. K.; Matyjaszewski, K. *Macromolecules* **2003**, *36*, 599−604.
(48) Buback, M.; Busch, M.; Lammel, R. A. *Macromol. Theory Simul.* **1996**, *5*, 845−861.
(49) van Berkel, K. Y.; Russell, G. T.; Gilbert, R. G. *Macromolecules* **2005**, *38*, 3214−3224.
(50) Castro, J. V.; van Berkel, K. Y.; Russell, G. T.; Gilbert, R. G. *Aust. J. Chem.* **2005**, *58*, 178−181.
(51) Jakubowski, W.; Matyjaszewski, K. *Macromolecules* **2005**, *38*, 4139−4146.
(52) Min, K.; Gao, H. F.; Matyjaszewski, K. *J. Am. Chem. Soc.* **2005**, *127*, 3825−3830.
(53) Jousset, S.; Qiu, J.; Matyjaszewski, K.; Granel, C. *Macromolecules* **2001**, *34*, 6641−6648.
(54) Sarbu, T.; Pintauer, T.; McKenzie, B.; Matyjaszewski, K. *J. Polym. Sci., Part A: Polym. Chem.* **2002**, *40*, 3153−3160.
(55) Gilbert, R. G. *Trends Polym. Sci.* **1995**, *3*, 222−226.
(56) Zetterlund, P. B.; Saka, Y.; McHale, R.; Nakamura, T.; Aldabbagh, F.; Okubo, M. *Polymer* **2006**, *47*, 7900−7908.

MA062786C